An approach in Minkowski space to hadron structure: the mock pion

Tobias Frederico
Instituto Tecnológico de Aeronáutica
São José dos Campos – Brazil
tobias@ita.br

Collaborators

W. de Paula (ITA), G. Salmè (INFN/Roma I), M. Viviani (INFN/Pisa), J. Carbonell (IPNO), V. Karmanov (Lebedev), E. Ydrefors (ITA), J. H. A. Nogueira(ITA/Roma I), C. Mezrag (INFN/Roma I), L. Tomio (ITA/IFT), J.P.B.C. Melo (UNICSUL)

Many Manifestations NonPerturbative QCD 2018
São Sebastião, April 30 – May 5, 2018.

Motivation

Physical space-time = Minkowski space

Develop methods in continuous nonperturbative QCD within a given dynamical simple framework

Solve the Bethe-Salpeter bound state equation

Observables: spectrum, SL/TL momentum region

Relation BSA to LF Fock-space expansion of the hadron wf

Problems to be addressed

Observables associated with the hadron structure in Minkowski Space obtainable from BSA

- parton distributions (pdfs)
- generalized parton distributions
- transverse momentum distributions (TMDs)
- Fragmentation functions
- SL and TL form factors ….
- Inversion Problem: Euclidean→Minkowski

TMDs & PDFs

FSI gluon exchange: T-odd

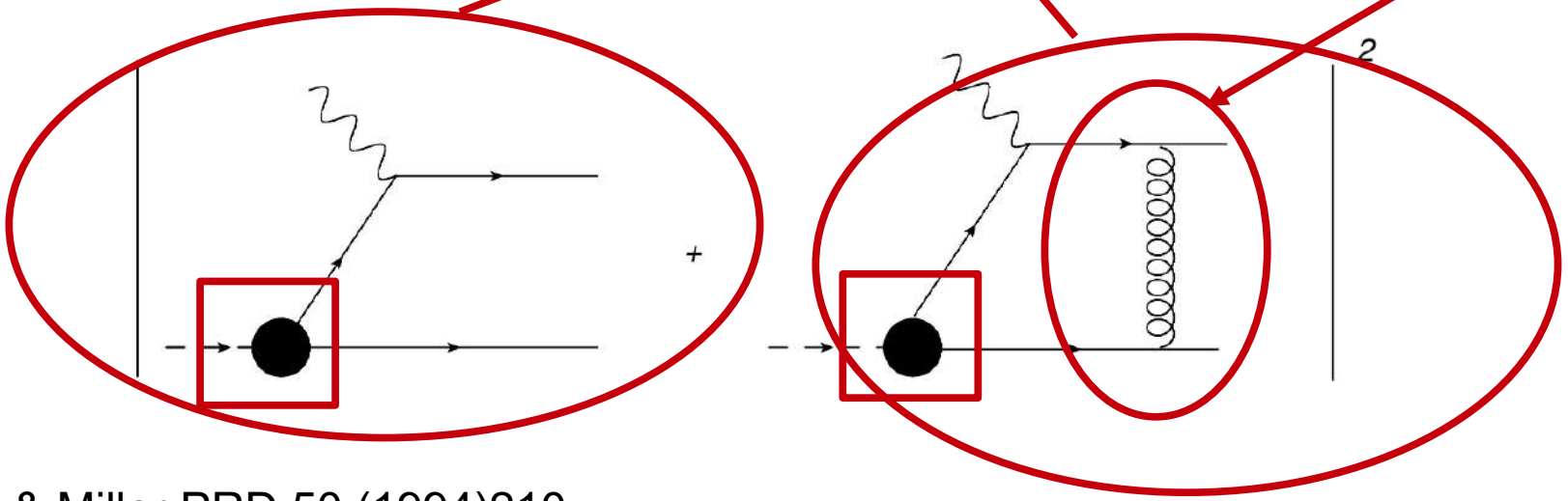

TF & Miller PRD 50 (1994)210

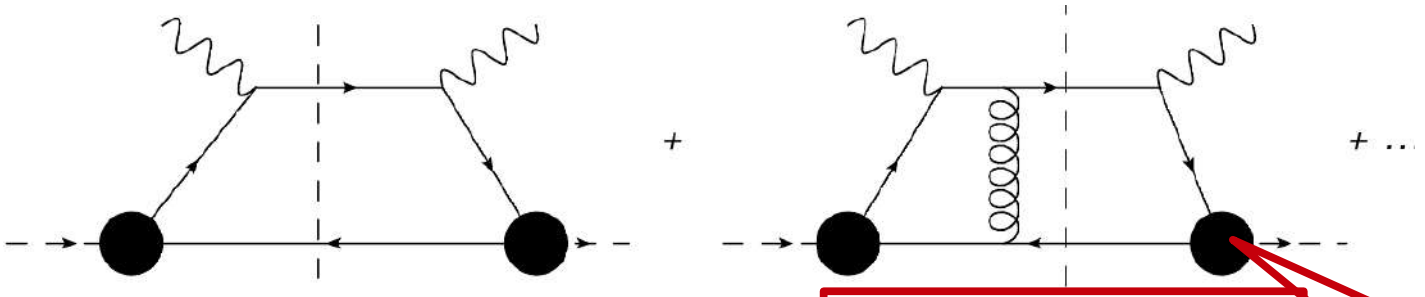

$q^2 = q^+q^- - q_T^2$

$q^+ = q^0+q^3$ $q^- = q^0-q^3$

$q^- \longrightarrow infty$

DIS

Bethe-Salpeter Amplitude @ $x^+=0$

Light-Front WF (LFWF)

basic ingredient in PDFs, GPDs and TMDs

$$\tilde{\Phi}(x,p) = \int \frac{d^4k}{(2\pi)^4} e^{ik\cdot x}\Phi(k,p)$$

$$p^\mu = p_1^\mu + p_2^\mu \qquad k^\mu = \frac{p_1^\mu - p_2^\mu}{2}$$

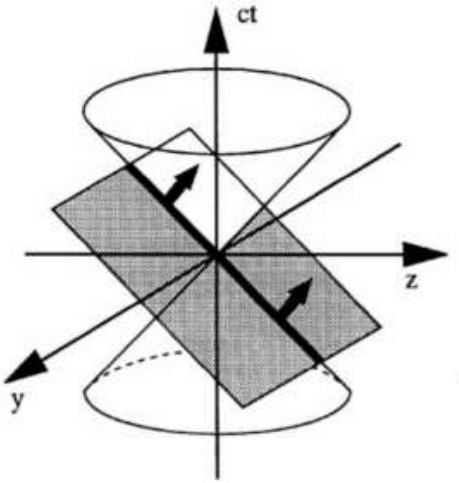

$$\tilde{\Phi}(x,p) = \langle 0|T\{\varphi_H(x^\mu/2)\varphi_H(-x^\mu/2)\}|p\rangle$$

$$= \theta(x^+)\langle 0|\varphi(\tilde{x}/2)e^{-iP^-x^+/2}\varphi(-\tilde{x}/2)|p\rangle e^{ip^-x^+/4} + \bullet\ \bullet\ \bullet$$

$$= \theta(x^+)\sum_{n,n'} e^{ip^-x^+/4}\langle 0|\varphi(\tilde{x}/2)|n'\rangle\langle n'|e^{-iP^-x^+/2}|n\rangle\langle n|\varphi(-\tilde{x}/2)|p\rangle + \bullet\ \bullet\ \bullet$$

$x^+ = 0$ only valence state remains! How to rebuilt the full BS amplitude?

Iterated Resolvents: Brodsky, Pauli, and Pinsky, Phys. Rep. 301, 299 (1998)

- **From the valence→ full Fock Space w-f:** Sales, et al. PRC61, 044003 (2000)

Main Tool: Nakanishi Integral Representation (NIR)

"Parametric representation for any Feynman diagram for interacting bosons, with a denominator carrying the overall analytical behavior in Minkowski space" (Nakanishi 1962)

Bethe-Salpeter amplitude

$$\Phi(k,p) = \int_{-1}^{1} dz' \int_{0}^{\infty} d\gamma' \frac{g(\gamma', z')}{(\gamma' + \kappa^2 - k^2 - p.kz' - i\epsilon)^3}$$

$$\kappa^2 = m^2 - \frac{M^2}{4}$$

BSE in Minkowski space with NIR for bosons

Kusaka and Williams, PRD 51 (1995) 7026;

Light-front projection: integration in k⁻

Carbonell&Karmanov EPJA27(2006)1;EPJA27(2006)11;

TF, Salme, Viviani PRD89(2014) 016010,…

Equivalent to Generalized Stietjes transform

Carbonell, TF, Karmanov PLB769 (2017) 418

LF wave function

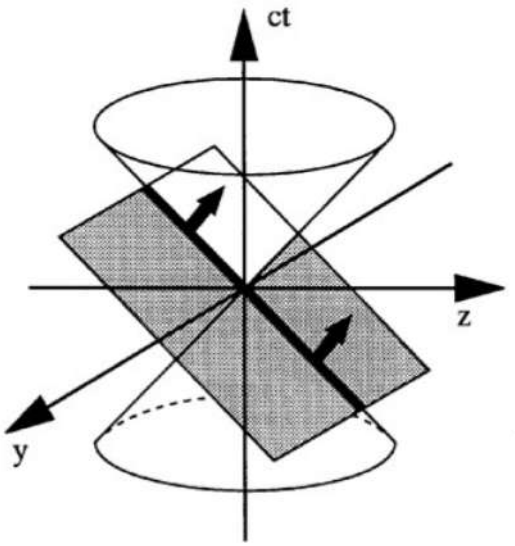

$$\psi_{LF}(\gamma, z) = \frac{1}{4}(1 - z^2) \int_0^\infty \frac{g(\gamma', z) d\gamma'}{\left[\gamma' + \gamma + z^2 m^2 + \kappa^2 (1 - z^2)\right]^2}$$

$$\gamma = k_\perp^2 \qquad z = 2x - 1$$

Two-Boson System: ground-state

Building a solvable model…

Nakanishi weight function

3+1 n=1

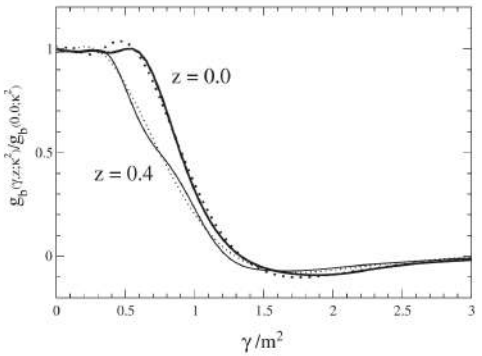

$\mu = 0.5 \;\; B/M = 1$

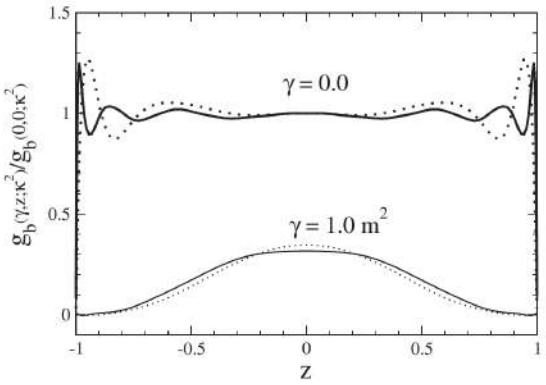

LADDER KERNEL

Valence wave function

3+1 n=1

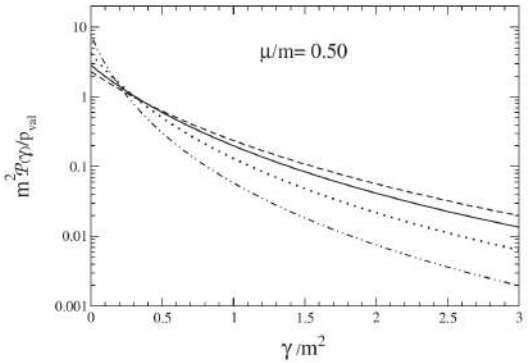

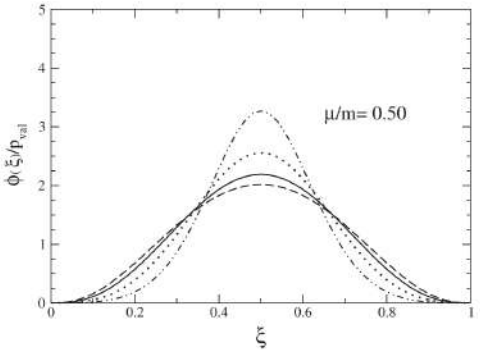

FIG. 3. The longitudinal LF distribution $\phi(\xi)$ for the valence component Eq. (34) vs the longitudinal-momentum fraction ξ for $\mu/m = 0.05,\ 0.15,\ 0.50$. Dash-double-dotted line: $B/m = 0.20$. Dotted line: $B/m = 0.50$. Solid line: $B/m = 1.0$. Dashed line: $B/m = 2.0$. Recall that $\int_0^1 d\xi\phi(\xi) = P_{val}$ (cf. Table III).

Karmanov, Carbonell, EPJA 27, 1 (2006)
Frederico, Salmè, Viviani PRD89, 016010 (2014)

(II) Valence LF wave function in impact parameter space

$$F(\xi, b)|_{b\to\infty} \to e^{-b\sqrt{\kappa^2+(\xi-1/2)^2M^2}}\, f(\xi, b)$$

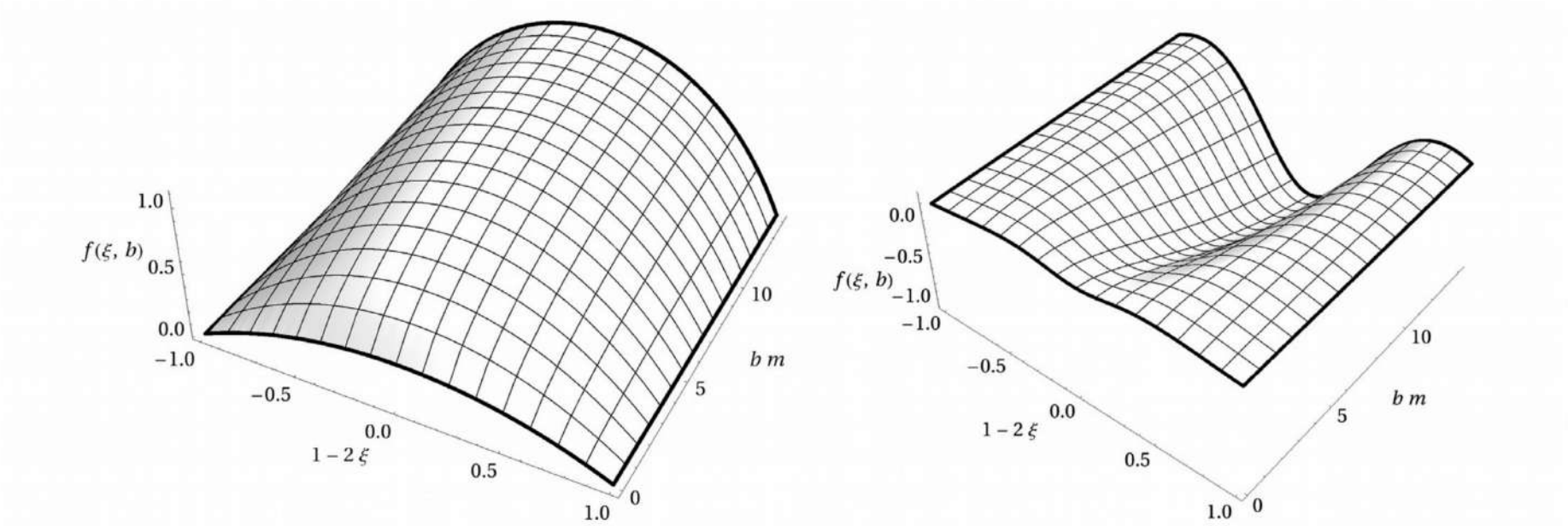

Fig. 7. The valence functions $f(\xi, b)$ in the impact parameter space. Left panel: the ground state, corresponding to $B(0) = 1.9m$, $\mu = 0.1m$ and $\alpha_{gr} = 6.437$. Right panel: first-excited state, corresponding to $B(1) = 0.22m$, $\mu = 0.1m$ and $\alpha_{gr} = 6.437$.

Gutierrez, Gigante, TF, Salmè,Viviani, Tomio PLB759 (2016) 131

Light-front valence wave function L+XL

Large momentum behavior

$$\psi_{LF}(\gamma,\xi) \to \alpha\ \gamma^{-2}\, C(\xi)$$

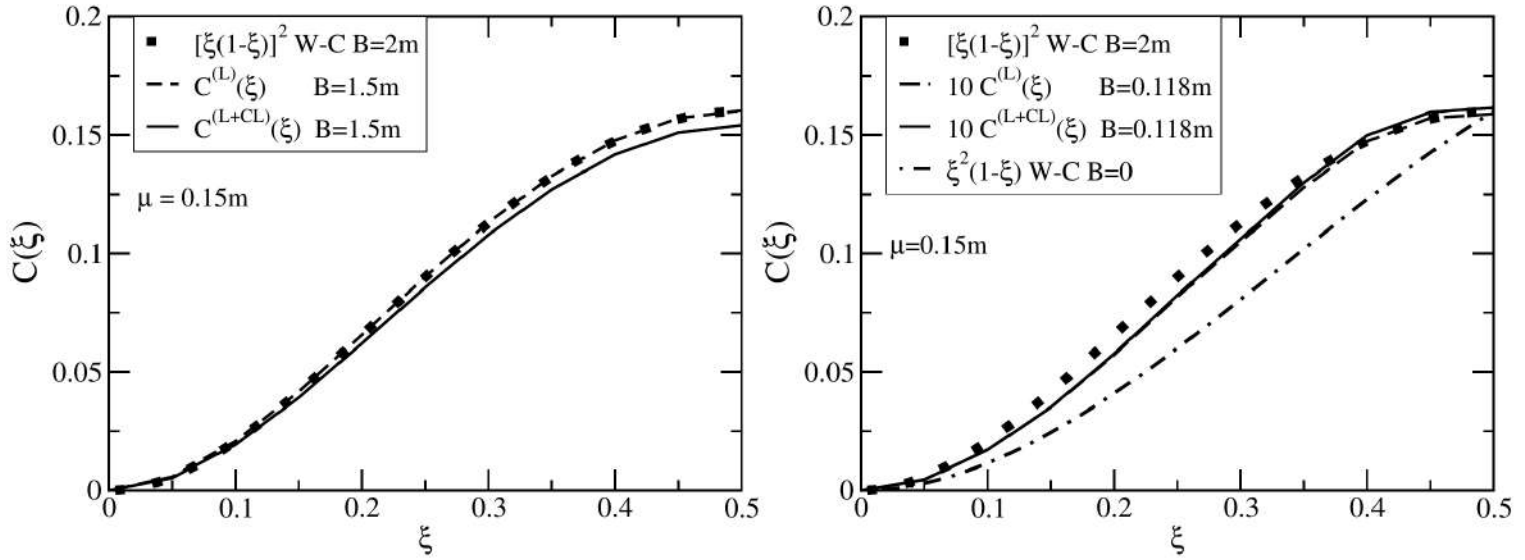

Fig. 2. Asymptotic function $C(\xi)$ defined from the LF wave function for $\gamma \to \infty$ (6) computed for the ladder kernel, $C^{(L)}(\xi)$ (dashed line), and ladder plus cross-ladder kernel, $C^{(L+CL)}(\xi)$ (solid line), with exchanged boson mass of $\mu = 0.15\,m$. Calculations are performed for $B = 1.5\,m$ (left frame) and $B = 0.118\,m$ (right frame). A comparison with the analytical forms of $C(\xi)$ valid for the Wick-Cutkosky model for $B = 2m$ (full box) and $B \to 0$ (dash-dotted line) both arbitrarily normalized.

Gigante, Nogueira, Ydrefors, Gutierrez, Karmanov, TF, PRD95(2017)056012.

Euclidean space: Nakanishi representation

Euclidean space (after the replacement $k_0 = ik_4$)

$$\Phi_E(k_v, k_4) = \int_{-1}^{1} dz' \int_0^{\infty} d\gamma' \frac{g(\gamma', z')}{\left(\gamma' + k_4^2 + k_v^2 + \kappa^2 - iMk_4 z'\right)^3}$$

$$k = (k_0, \vec{k}) \qquad \kappa^2 = m^2 - \frac{M^2}{4}$$

- Note: Wick-rotation is the exact analytical continuation of the Minkowski space Nakanishi representation of the BS amplitude!

Transverse distribution: Euclidean and Minkowski

$$\phi_M^T(\mathbf{k}_\perp) \equiv \int dk^0 dk^3 \Phi(k,p) = \frac{1}{2}\int dk^+ dk^- \Phi(k,p) \text{ and}$$

$$\phi_E^T(\mathbf{k}_\perp) \equiv \mathrm{i}\int dk_E^0 dk^3 \Phi_E(k_E,p),$$

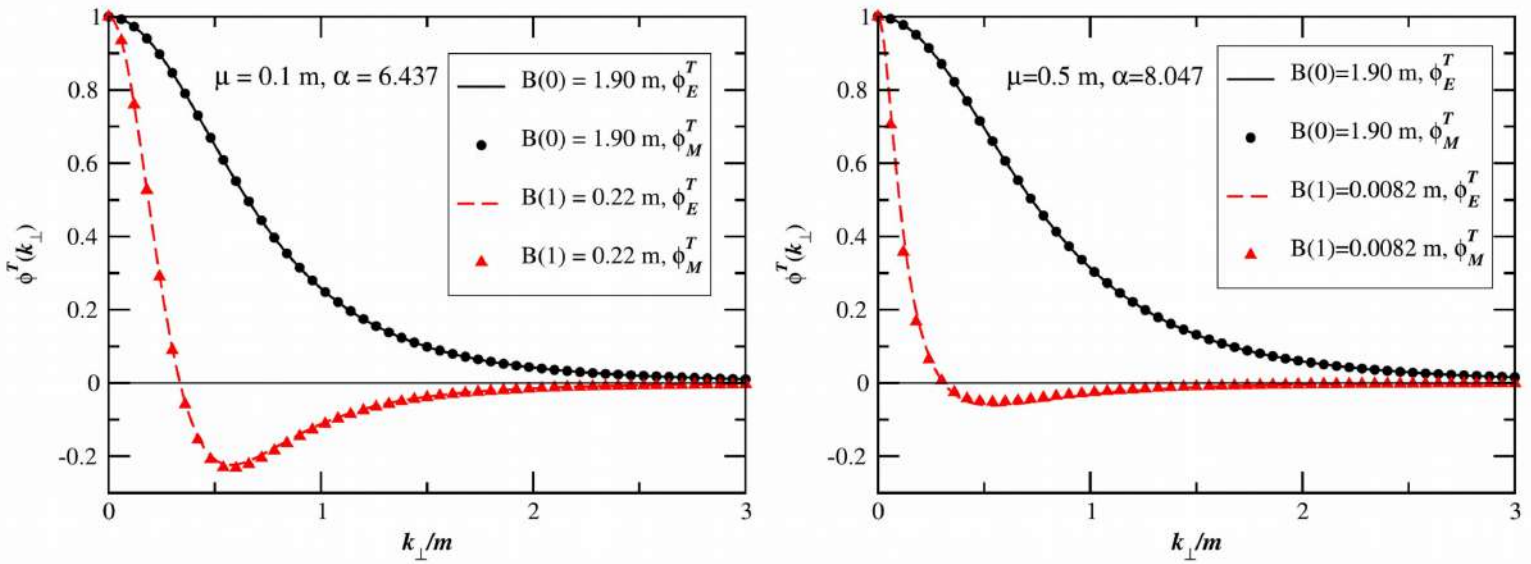

Fig. 6. Transverse momentum amplitudes s-wave states, in Euclidean and Minkowski spaces, vs $k_\perp$, for both ground- and first-excited states, and two values of μ/m and α_{gr} (as indicated in the insets). The amplitudes ϕ_E^T and ϕ_M^T, arbitrarily normalized to 1 at the origin, are not easily distinguishable.

Gutierrez, Gigante, TF, Salmè,Viviani, Tomio PLB759 (2016) 131

GOAL

Invert the Nakanishi Representation

Carbonell, TF, Karmanov, Eur. Phys. J. C 77, 58 (2017)

$$\Phi_E \longrightarrow g_E \longrightarrow \Phi_M$$

Lattice & Euclidean BS [Chang et al PRL110(2013)132001]

$$\psi_{LF} \longrightarrow g_{LF} \longrightarrow \Phi_M$$

LF Quantization & Models

$$\Phi_M \Longrightarrow$$ ***Observables***

Nakanishi representation

Euclidean BS amplitude

$$\Phi_E(k_v, k_4) = \int_{-1}^{1} dz' \int_0^{\infty} d\gamma' \frac{g(\gamma', z')}{(\gamma' + k_4^2 + k_v^2 + \kappa^2 - iMk_4 z')^3}$$

$$\Phi_E = K_E\, g$$

LF valence W-F

$$\psi_{LF}(\gamma, z) = \frac{1}{4}(1 - z^2) \int_0^{\infty} \frac{g(\gamma', z) d\gamma'}{\left[\gamma' + \gamma + z^2 m^2 + \kappa^2(1 - z^2)\right]^2}$$

$$\gamma = k_\perp^2$$

$$z = 2x - 1$$

$$\psi_{LF} = L\, g$$

Mapping

$$0 < \gamma', k_v, k_4 < \infty \quad \rightarrow \quad 0 < x', x, z < 1$$

$$\gamma' = \frac{x'}{1-x'}, \quad k_v = \frac{x}{1-x}, \quad k_4 = \frac{z}{1-z}$$

Euclidian BS amplitude

$$\Phi_E(x,z) = \int_0^1 dx' \int_0^1 dz'\, K(x,z;x',z') g(x',z')$$

$$K(x,z;x',z') = \mathrm{Re}\left[\frac{2}{\left(\frac{x^2}{(1-x)^2} + \frac{z^2}{(1-z)^2} + \frac{x'}{1-x'} + \kappa^2 - iM\frac{zz'}{1-z}\right)^3}\right] \frac{1}{(1-x')^2}$$

$$g(-z',x') = g(z',x')$$

LF wave function **&** **Mapping**

$$\psi_{LF}(x,z) = \int_0^1 dx'\, L(x,x';z) g(z,x')$$

$$L(x,x';z) = \frac{(1-z^2)}{4\left(\frac{x}{1-x} + \frac{x'}{1-x'} + z^2 m^2 + \kappa^2(1-z^2)\right)^2 (1-x')^2}$$

$$x = \frac{\gamma}{1+\gamma} \qquad x' = \frac{\gamma'}{1+\gamma'}$$

z plays role of a parameter

Solving equations $\Phi_E \rightarrow g_E$

$$g(x,z) = \sum_{i,j=1}^{N_x,N_z} c_{ij} G_{i-1}(x) G_{j-1}(z)$$

Gegenbauer polynomial

$$\int_0^1 dx\, G_n(x) G_{n'}(x) = \delta_{nn'} \qquad G_n(x) = \sqrt{2n+1}\, C_n^{\left(\frac{1}{2}\right)}(2x-1)$$

$$\Phi_{ij} = \sum_{i'j'}^{N_z,N_x} K_{ij}^{i'j'} c_{i'j'}$$

$$\Phi_{ij} = \Phi_E(x_i, z_j), \qquad K_{ij}^{i'j'} = \int_0^1 dz' \int_0^1 dx'\, K(x_i, z_j; z', x') G_{i'-1}(x') G_{j'-1}(z')$$

validate equation in $N_x \times N_z$ discrete points x_i, z_j

Gaussian-Legendre points

Solving equations $\psi_{LF} \rightarrow g_{LF}$

$$g(x,z) = \sum_{i=1}^{N} c_i G_{i-1}(x)$$

z plays role of a parameter

$$\psi_{LF}(x_j) = \sum_{i=1}^{N} L_{ji}\, c_i$$

$$L_{ji} = \int_0^1 dx'\, L(x_j, x'; z)\, G_{i-1}(x')$$

Solution of an ill-posed problem $A\,C \;=\; B$ ***!!!!?***

Tikhonov regularization method

A.N. Tikhonov, A.V. Goncharsky, V.V. Stepanov, A.G. Yagola, *Numerical Methods for the Solution of Ill-Posed Problems*, Kluwer Academic Publishers, 1995.

$\| AC - B \|$ minimization problem

$$A^\dagger AC + \epsilon C = A^\dagger B \quad \Rightarrow \quad C_\epsilon = (A^\dagger A + \epsilon I)^{-1} A^\dagger B$$

with $\epsilon \ll 1$

naive form $\quad C_\epsilon = (A + \epsilon I)^{-1} B$

OBE interaction Two-boson bound state &Ladder Kernel

$$\Phi_E \rightarrow g_E$$

Tikhonov reg.

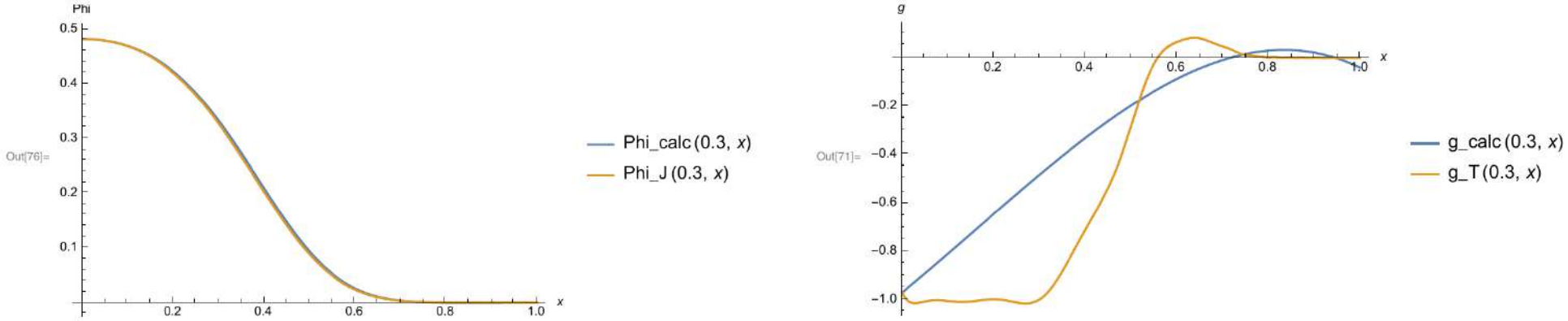

Fig. 4. *Left-frame:* the yellow curve corresponds to the Euclidean BS amplitude $c_2\,\Phi_E(z = 0.3, x)$ $(c_2 = 0.88)$ calculated via BS equation with the OBE kernel [12]. The blue curve corresponds to the amplitude, calculated via g by Eq. (6). *Right-frame:* the solution $c\,g_E(x,\, z = 0.3)$ (blue) found solving Eq. (6) with $N_z = 2, N_x = 4$ and $\epsilon = 10^{-10}$, with Φ_E [12], using the Tikhonov regularization method, compared to the solution $g_{FSV}(x,\, z = 0.3)$ [5,11] (yellow).

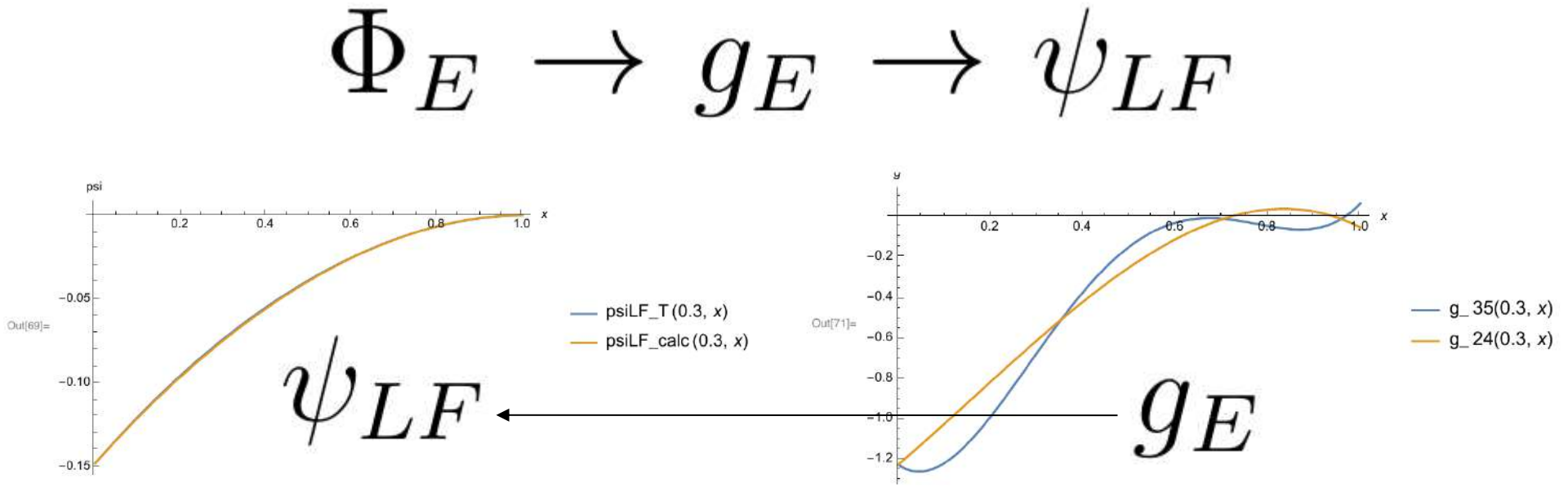

Fig. 5. *Left-frame:* LF wave function calculated by Eq. (8) and renormalized as $c_1\,\psi_{LF}(x, z = 0.3)$ for both extracted g's (the two ψ_{LF} overlaps within the width of the blue curve) and compared to the actual results obtained with g_{FSV} [5,11] (yellow curve) from the Minkowski space solution of the BS equation. *Right-frame:* $g(x, z = 0.3)$ extracted from Φ_E, with $N_z = 2$, $N_x = 4$ and $N_x = 5$, $N_z = 3$ with $\epsilon = 10^{-10}$ using Tikhonov regularization method.

Calculating EM form factor

$$(p+p')^\nu F^{BSM}(Q^2) =$$
$$i\int \frac{d^4k}{(2\pi)^4}(p+p'-2k)^\nu(k^2-m^2)\,\Phi_M\left(\frac{1}{2}p-k;p\right)\Phi_M\left(\frac{1}{2}p'-k;p'\right)$$

$$F^{BSM}(Q^2) = \frac{1}{2^7\pi^3 N_{BSM}}\int_0^\infty d\gamma\int_{-1}^1 dz\, g(\gamma,z)$$
$$\times\int_0^\infty d\gamma'\int_{-1}^1 dz'\, g(\gamma',z')\int_0^1 du\, u^2(1-u)^2\frac{f_{num}}{f_{den}^4}$$

J. Carbonell, V.A. Karmanov, M. Mangin-Brinet, Eur. Phys. J. A **39**, 53 (2009)

$$f_{num} = (6\xi-5)m^2 + [\gamma'(1-u)+\gamma u](3\xi-2) + 2M^2\xi(1-\xi) +$$
$$+\frac{1}{4}Q^2(1-u)u(1+z)(1+z')$$

$$f_{den} = m^2 + \gamma'(1-u) + \gamma u - M^2(1-\xi)\xi + \frac{1}{4}Q^2(1-u)u(1+z)(1+z')$$

Valence contribution:

$$F^{LF}(Q^2) = \frac{1}{(2\pi)^3} \int \psi_{LF}(\vec{k}_\perp, x)\psi_{LF}(\vec{k}_\perp - x\vec{Q}_\perp, x) \frac{d^2k_\perp dx}{2x(1-x)}$$

$$F^{LF}(Q^2) = \frac{1}{2^5\pi^3 N_{LF}} \int_0^\infty d\gamma' \int_0^\infty d\gamma \int_0^1 dx \int_0^1 du \times \frac{x(1-x)\,u(1-u)\,g(\gamma, 2x-1)g(\gamma', 2x-1)}{[u\gamma + (1-u)\gamma' + u(1-u)x^2Q^2 + m^2 - x(1-x)M^2]^3}$$

J. Carbonell, V.A. Karmanov, M. Mangin-Brinet, Eur. Phys. J. A **39**, 53,(2009)

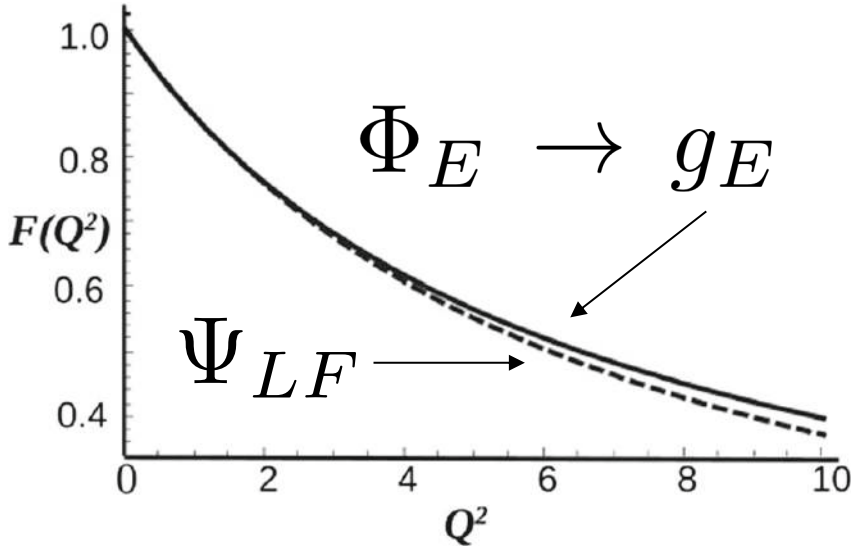

Fig. 10 EM form factor calculated via LF wave function by Eq. (31), for $N_z = 2,\ N_x = 4$ (*dashed curve*) and for $N_z = 3$, $N_x = 5$ (*solid curve*), i.e., via solutions g_E shown Fig. 9

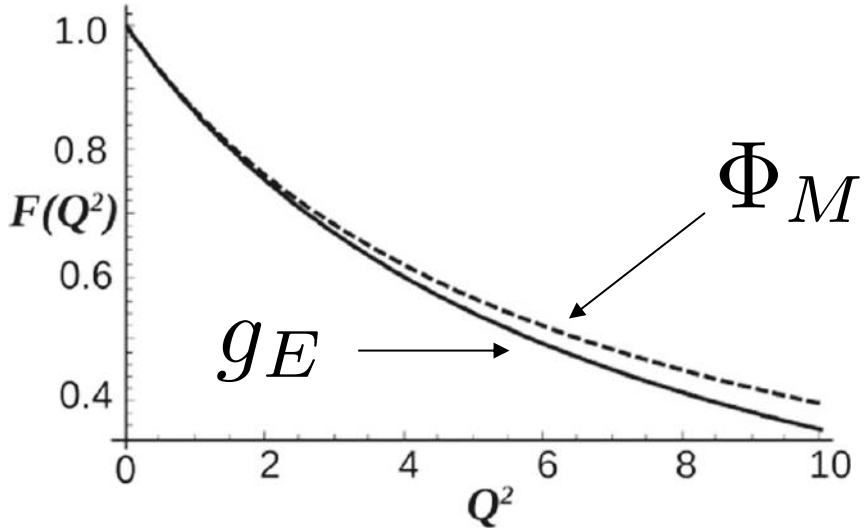

Fig. 11 EM form factor calculated via Minkowski BS amplitude, by Eq. (29) with the same g_E used to calculate the *curves* in Fig. 10; the *curves* are indicated as in Fig. 10

Stability of the observables: weighting by the small eigenvalues of the corresponding eigenstates in the Minkowski BS amplitude

SUMMARY: INV METHOD

- Extract Nakanishi weight function with
Tikhonov regularization + mapping + expansion

- from valence LF wave function is stable

- from Euclidean BS amplitude some residual instability

- from Euclidean BS to LF wave function/ Form Factor
shows some stability

Generalized Stietjes transform and the LF valence wave function

Jaume Carbonell, TF, Vladimir Karmanov PLB769 (2017) 418

$$\psi_{LF}(\gamma, z) = \frac{1-z^2}{4} \int_0^\infty \frac{g(\gamma', z)d\gamma'}{\left[\gamma' + \gamma + z^2 m^2 + (1-z^2)\kappa^2\right]^2}.$$

$$f(\gamma) \equiv \int_0^\infty d\gamma'\, L(\gamma, \gamma') g(\gamma') = \int_0^\infty d\gamma'\, \frac{g(\gamma')}{(\gamma' + \gamma + b)^2}$$

denoted symbolically as $f = \hat{L}\, g$.

$$g(\gamma) = \hat{L}^{-1} f = \frac{\gamma}{2\pi} \int_{-\pi}^{\pi} d\phi\; e^{i\phi}\, f(\gamma\, e^{i\phi} - b).$$

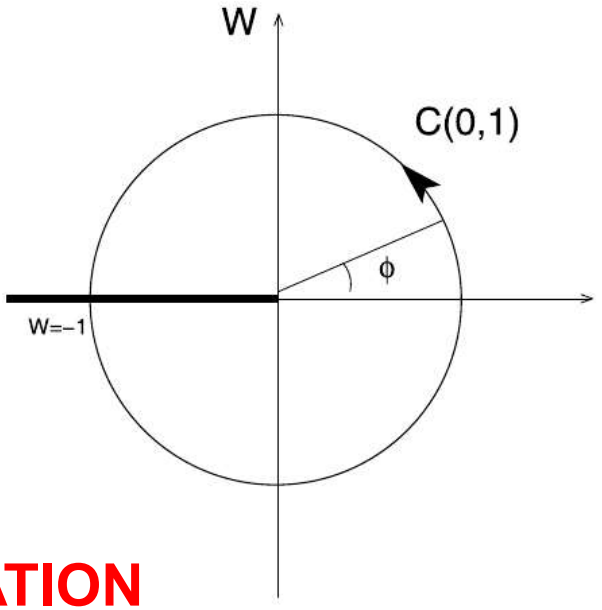

J.H. Schwarz, J. Math. Phys. 46 (2005) 014501,

UNIQUENESS OF THE NAKANISHI REPRESENTATION

PHENOMENOLOGICAL APPLICATIONS from the valence wf → BSA!

BSE for qqbar: pion

Carbonell and Karmanov EPJA 46 (2010) 387;

de Paula, TF,Salmè, Viviani PRD 94 (2016) 071901;

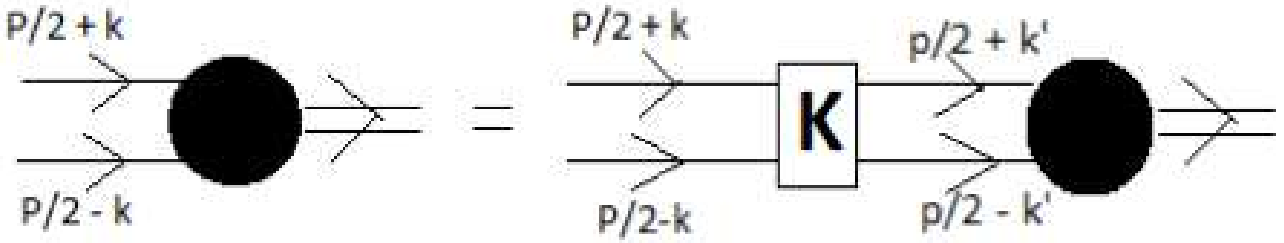

$$\Phi(k,p) = S(k+p/2) \int \frac{d^4k'}{(2\pi)^4} F^2(k-k')\, i\mathcal{K}(k,k')\, \Gamma_1\, \Phi(k',p)\, \bar{\Gamma}_2\, S(k-p/2)$$

Ladder approximation (L): suppression of XL for Nc=3 [A. Nogueira, CR Ji, Ydrefors, TF, PLB(2017) 1710.04398 [hep-th]]

Vector $$i\mathcal{K}_V^{(Ld)\mu\nu}(k,k') = -ig^2 \frac{g^{\mu\nu}}{(k-k')^2 - \mu^2 + i\epsilon}$$

Vertex Form-Factor $$F(q) = \frac{\mu^2 - \Lambda^2}{q^2 - \Lambda^2 + i\epsilon}$$

NIR for fermion-antifermion: 0^- (pion)

BS amplitude

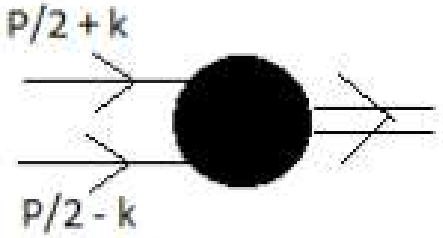

$$\Phi(k,p) = S_1\phi_1 + S_2\phi_2 + S_3\phi_3 + S_4\phi_4$$

$$S_1 = \gamma_5 \quad S_2 = \frac{1}{M}\not{p}\gamma_5 \quad S_3 = \frac{k\cdot p}{M^3}\not{p}\gamma_5 - \frac{1}{M}\not{k}\gamma_5 \quad S_4 = \frac{i}{M^2}\sigma_{\mu\nu}p^\mu k^\nu\gamma_5$$

$$\phi_i(k,p) = \int_{-1}^{+1} dz' \int_0^\infty d\gamma' \frac{g_i(\gamma',z')}{(k^2 + p\cdot k\; z' + M^2/4 - m^2 - \gamma' + i\epsilon)^3}$$

Light-front projection: integration over k^- (LF singularities)

For the two-fermion BSE, singularities have generic form:

$$\mathcal{C}_j = \int_{-\infty}^{\infty} \frac{dk^-}{2\pi} (k^-)^j \; \mathcal{S}(k^-, v, z, z', \gamma, \gamma') \qquad j = 1, 2, 3$$

with $\mathcal{S}(k^-, v, z, z', \gamma, \gamma')$ explicitly calculable

N.B., in the worst case

$$\mathcal{S}(k^-, v, z, z', \gamma, \gamma') \sim \frac{1}{[k^-]^2} \qquad \text{for} \quad k^- \to \infty$$

End-point singularities: T.M. Yan , Phys. Rev. **D 7**, 1780 (1973)

$$\mathcal{I}(\beta, y) = \int_{-\infty}^{\infty} \frac{dx}{\Big[\beta x - y \mp i\epsilon\Big]^2} = \pm \frac{2\pi i \; \delta(\beta)}{\Big[-y \mp i\epsilon\Big]}$$

→ Kernel with delta's and its derivatives!

End-point singularities– more intuitive: can be treated by the pole-dislocation method de Melo et al. NPA631 (1998) 574C, PLB708 (2012) 87

Numerical comparison: Scalar coupling

	$\mu/m = 0.15$			$\mu/m = 0.50$		
B/m	g^2_{dFSV}(full)	g^2_{CK}		g^2_{dFSV}(full)	g^2_{CK}	g^2_E
0.01	7.844	7.813		25.327	25.23	-
0.02	10.040	10.05		29.487	29.49	-
0.04	13.675	13.69		36.183	36.19	36.19
0.05	15.336	15.35		39.178	39.19	39.18
0.10	23.122	23.12		52.817	52.82	-
0.20	38.324	38.32		78.259	78.25	-
0.40	71.060	71.07		130.177	130.7	130.3
0.50	88.964	86.95		157.419	157.4	157.5
1.00	187.855	-		295.61	-	-
1.40	254.483	-		379.48	-	-
1.80	288.31	-		421.05	-	-

First column: binding energy.

Red digits: coupling constant g^2 for $\mu/m = 0.15$ and 0.50, with the analytical treatment of the fermionic singularities (present work). -

Black digits: results for $\mu/m = 0.15$ and 0.50, with a numerical treatment of the singularities (Carbonell & Karmanov EPJA **46**, (2010) 387).

Blue digits: results in Euclidean space from Dorkin et al FBS. **42** (2008) 1.

Scalar boson exchange

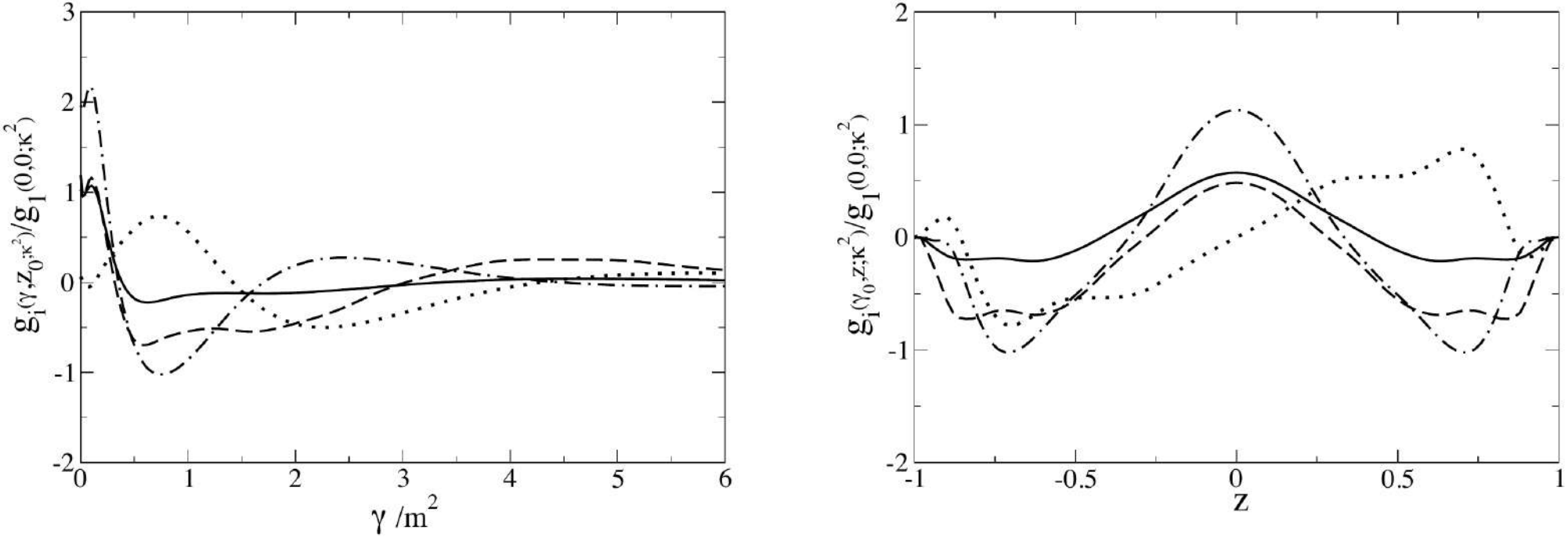

Figure 2. Nakanishi weight-functions $g_i(\gamma,\, z; \kappa^2)$, Eqs. 3.1 and 3.2 evaluated for the 0^+ two-fermion system with a scalar boson exchange such that $\mu/m = 0.5$ and $B/m = 0.1$ (the corresponding coupling is $g^2 = 52.817$ [17]). The vertex form-factor cutoff is $\Lambda/m = 2$. Left panel: $g_i(\gamma,\, z_0; \kappa^2)$ with $z_0 = 0.6$ and running γ/m^2. Right panel: $g_i(\gamma_0,\, z; \kappa^2)$ with $\gamma_0/m^2 = 0.54$ and running z, The Nakanishi weight-functions are normalized with respect to $g_1(0, 0; \kappa^2)$. Solid line: g_1. Dashed line: g_2. Dotted line: g_3. Dot-dashed line: g_4.

de Paula, TF,Salmè, Viviani PRD 94 (2016) 071901;

Massless vector exchange: high-momentum tails

de Paula, TF,Salmè, Viviani PRD 94 (2016) 071901;

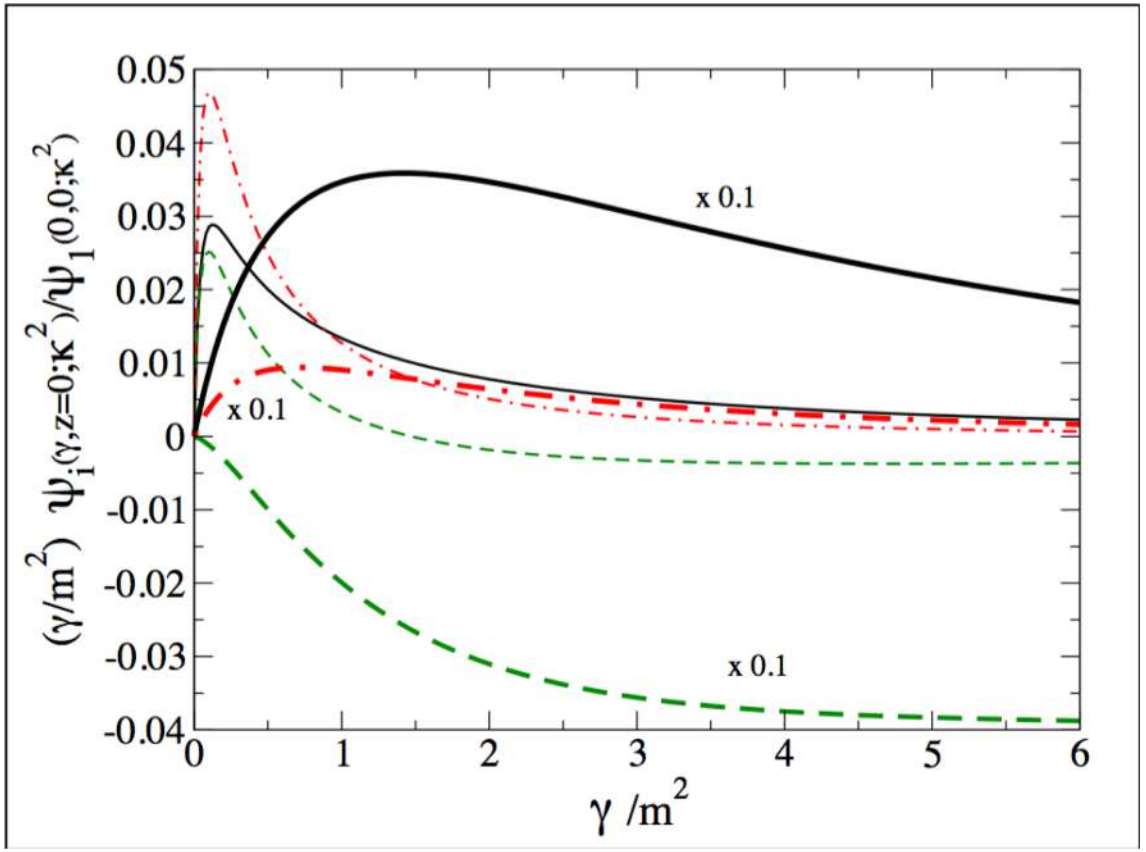

LF amplitudes ψ_i times γ/m^2 at fixed $z = 0$, for the vector coupling.
$B/m = 0.1$ (thin lines) and 1.0 (thick lines).

——— : $(\gamma/m^2)\ \psi_1$.
– – : $(\gamma/m^2)\ \psi_2$.
– • : $(\gamma/m^2)\ \psi_4$.
$\psi_3 = 0$ for $z = 0$

Power one is expected for the pion valence amplitude:

X Ji et al, PRL 90 (2003) 241601.

PION MODEL

W. de Paula, TF, Pimentel, Salmè, Viviani, EPJC 77 (2017) 764

- **Gluon effective mass ~ 500 MeV – Landau Gauge LQCD**

[Oliveira, Bicudo, JPG 38 (2011) 045003;
Duarte, Oliveira, Silva, Phys. Rev. D 94 (2016) 01450240]

- **Mquark = 250 MeV**

[Parappilly, et al, PR D73 (2006) 054504]

- **Λ/m =1, 2, 3**

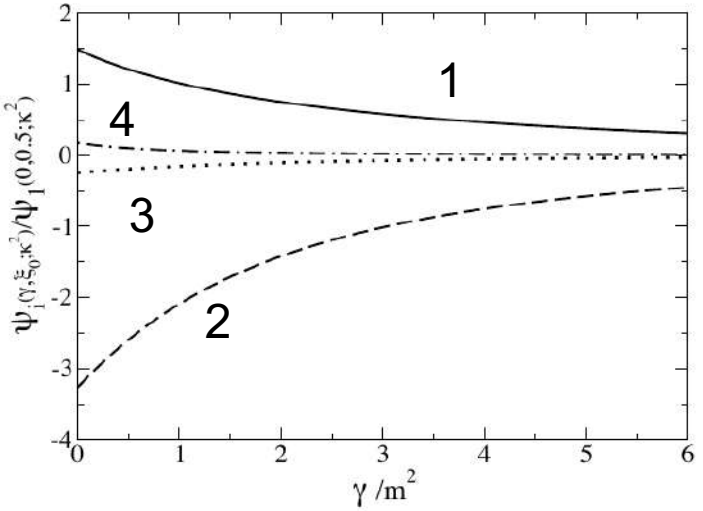

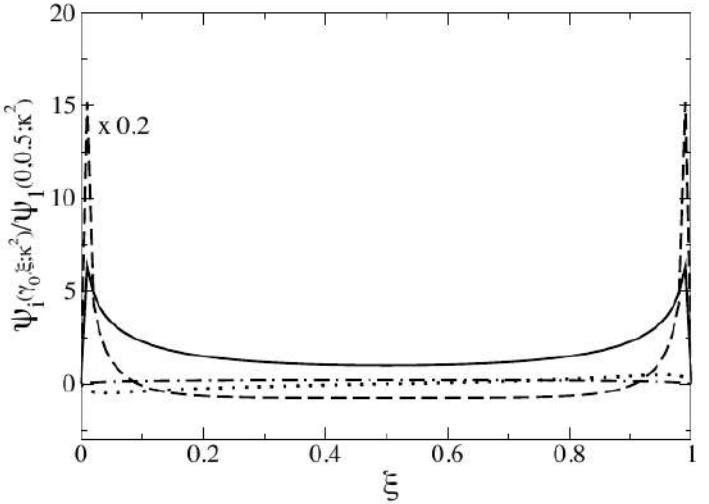

twist 3 DA

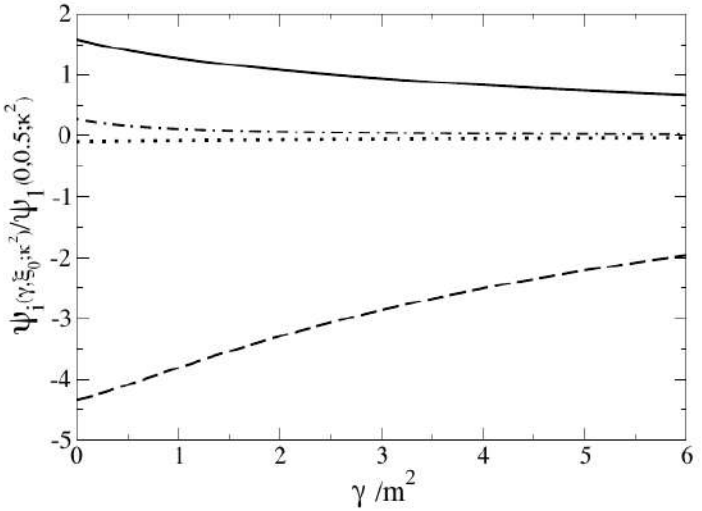

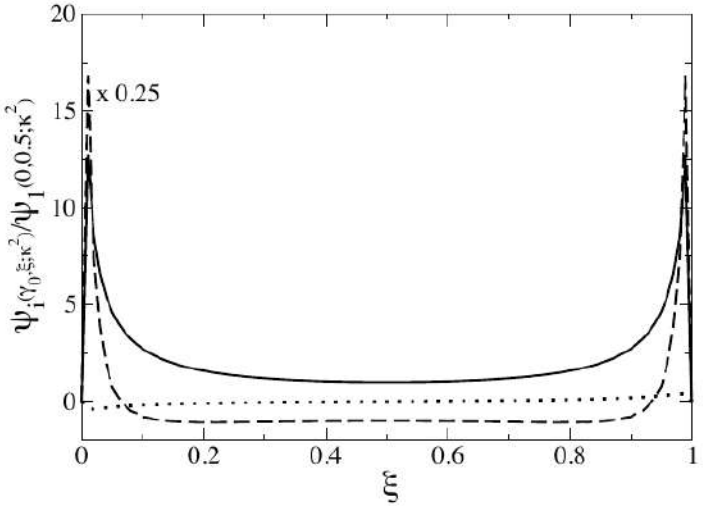

$f_\pi = 150\,\mathrm{MeV}$

Figure 6. Light-front amplitudes $\psi_i(\gamma, \zeta)$, Eq. 3.11, for the pion-like system with a heavy-vector exchange ($\mu/m = 2$), binding energy of $B/m = 1.44$ and constituent mass $m = 250$ MeV. Upper panel: vertex form-factor cutoff $\Lambda/m = 3$ and $g^2 = 435.0$, corresponding to $\alpha_s = 10.68$ (see text for the definition of α_s). Lower panel: vertex form-factor cutoff $\Lambda/m = 8$ and $g^2 = 53.0$, corresponding to $\alpha_s = 3.71$. The value of the longitudinal variable is $\xi_0 = 0.2$ and $\gamma_0 = 0$. Solid line: ψ_1 . Dashed line: ψ_2. Dotted line: ψ_3. Dot-dashed line: ψ_4

Valence distribution functions

W. de Paula, et. al, in preparation

Valence probability:

$$N_2 = \frac{1}{32\,\pi^2}\int_{-1}^{1} dz \int_0^{\infty} d\gamma \left\{ \tilde{\psi}_{val}(\gamma,\xi)\ \tilde{\psi}_{val}(\gamma,\xi) + \frac{\gamma}{M^2}\ \psi_{val;4}(\gamma,\xi)\ \psi_{val;4}(\gamma,\xi) \right\}$$

$$\tilde{\psi}_{val}(\gamma,z) = -\frac{i}{M}\int_0^{\infty} d\gamma' \frac{g_2(\gamma',z)}{[\gamma+\gamma'+m^2z^2+(1-z^2)\kappa^2-i\epsilon]^2}$$
$$-\frac{i}{M}\frac{z}{2}\int_0^{\infty} d\gamma' \frac{g_3(\gamma',z)}{[\gamma+\gamma'+m^2z^2+(1-z^2)\kappa^2-i\epsilon]^2}$$
$$+\frac{i}{M^3}\int_0^{\infty} d\gamma' \frac{\partial g_3(\gamma',z)/\partial z}{[\gamma+\gamma'+z^2m^2+(1-z^2)\kappa^2-i\epsilon]}$$

$$\psi_{val;4}(\gamma,z) = -\frac{i}{M}\int_0^{\infty} d\gamma' \frac{g_4(\gamma',z)}{[\gamma+\gamma'+m^2z^2+(1-z^2)\kappa^2-i\epsilon]^2}\,.$$

Valence probability

Table 1 Valence probability for a massive vector exchange, with $\mu/m = 0.15$ and a cut-off $\Lambda/m = 2$ for the vertex form-factor. The number of gaussian points is 72.

B/m	Prob.
0.01	0.48
0.1	0.39
1.0	0.34

Table 2 Valence probability for a massive vector exchange, with $\mu/m = 0.5$ and a cut-off $\Lambda/m = 2$ for the vertex form-factor. The number of gaussian points is 72.

B/m	Prob.
0.01	0.48
0.1	0.42
1.0	0.34

Lot of room for the higher LF Fock components of the wave function to manifest!

Valence distribution functions: longitudinal and transverse

Mquark 187 MeV

Mgluon 28 MeV

Λ/m =2

P_val=0.32

$f_\pi = 77\,\mathrm{MeV}$

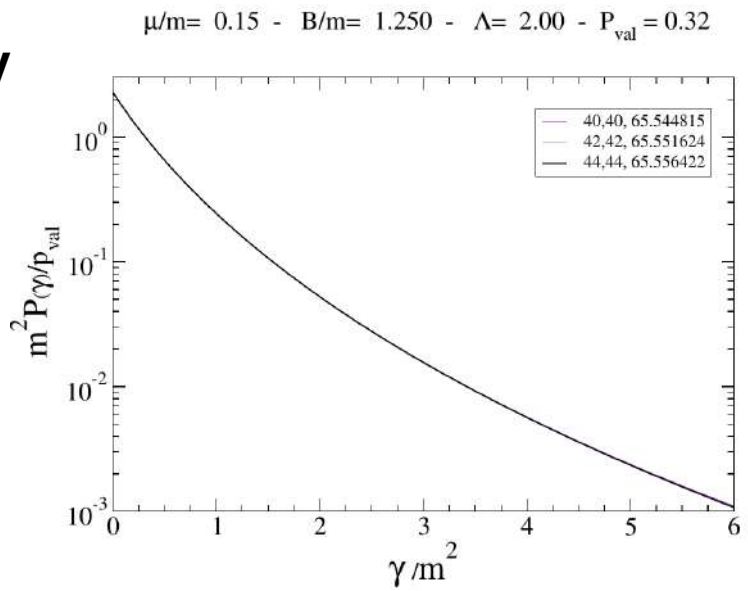

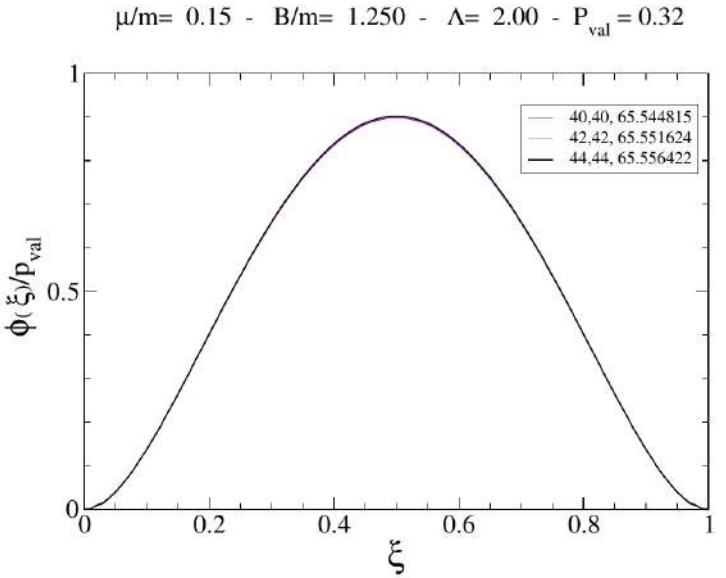

Mquark 187 MeV

Mgluon 280 MeV

Λ/m =2

P_val=0.39

$f_\pi = 99\,\mathrm{MeV}$

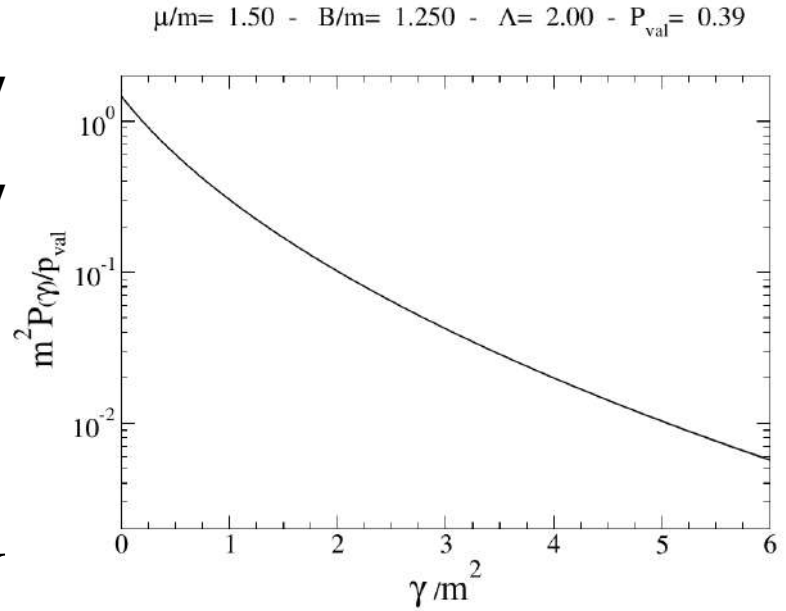

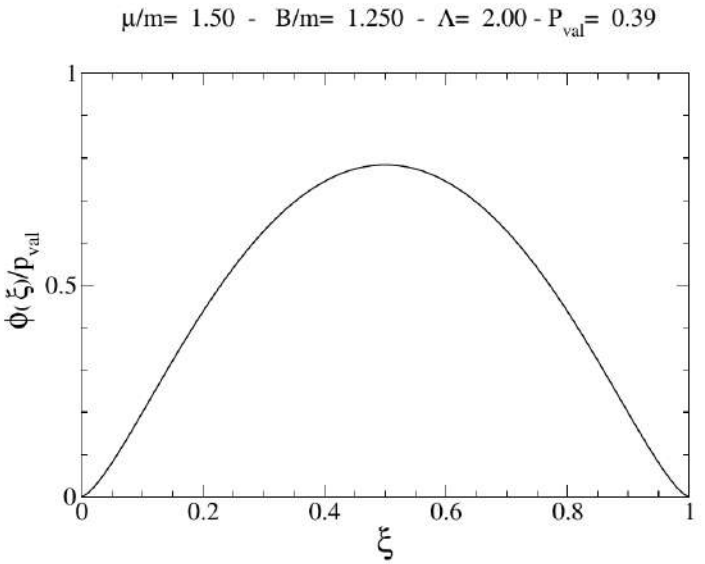

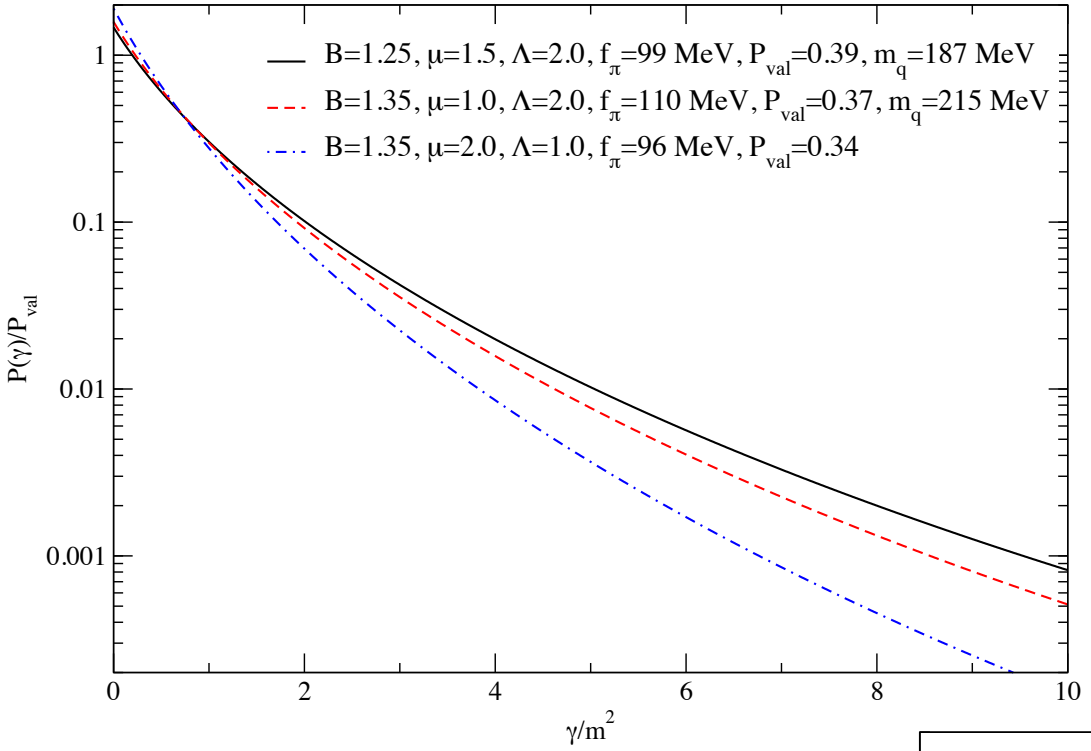
B=1.25, μ=1.5, Λ=2.0, f_π=99 MeV, P_val=0.39, m_q=187 MeV
B=1.35, μ=1.0, Λ=2.0, f_π=110 MeV, P_val=0.37, m_q=215 MeV
B=1.35, μ=2.0, Λ=1.0, f_π=96 MeV, P_val=0.34
P(γ)/P_val
γ/m^2
1
0.1
0.01
0.001
0
2
4
6
8
10

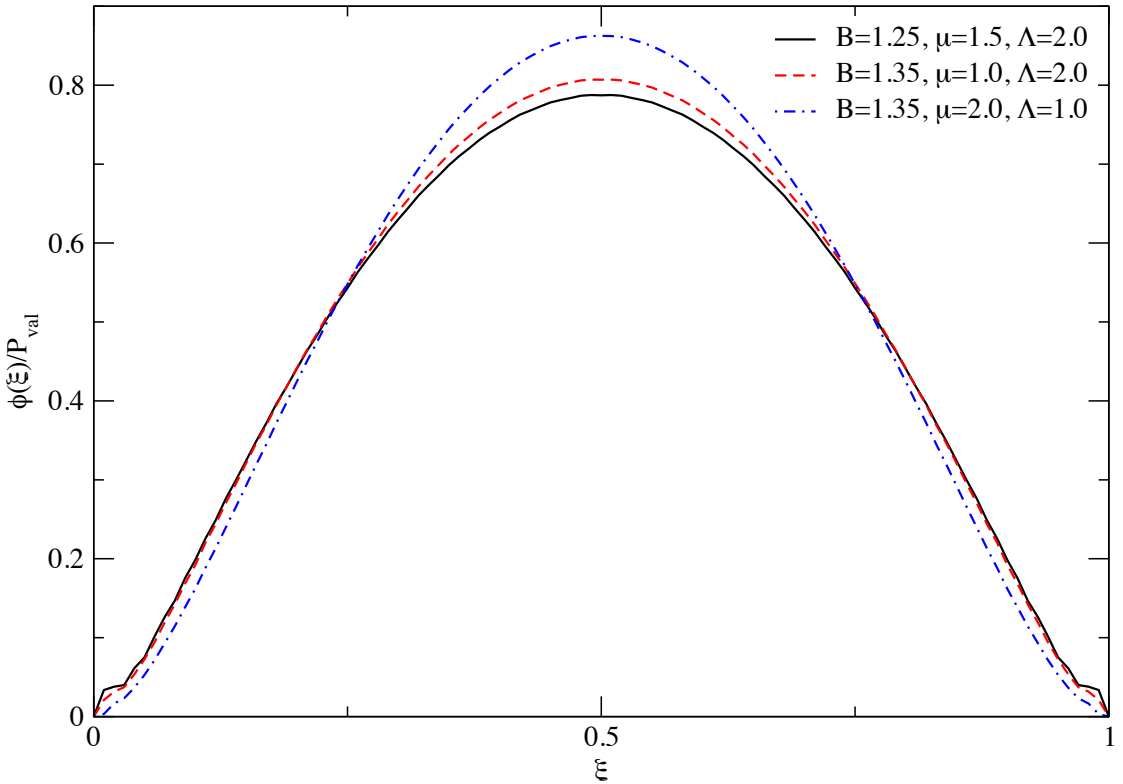
B=1.25, μ=1.5, Λ=2.0
B=1.35, μ=1.0, Λ=2.0
B=1.35, μ=2.0, Λ=1.0
φ(ξ)/P_val
ξ
0.8
0.6
0.4
0.2
0
0
0.5
1

Preliminary result for a fermion-scalar bound system

The covariant decomposition of the BS amplitude for a $(1/2)^+$ bound system, composed by a fermion and a scalar, reads

$$\Phi(k,p) = \Big[S_1\ \phi_1(k,p) + S_2\ \phi_2(k,p)\Big]\ U(p,s)$$

with $U(p,s)$ a Dirac spinor, $S_1(k) = 1$, $S_2(k) = \not{k}/M$,and $M^2 = p^2$

A first check: scalar coupling $\alpha^s = \lambda_F^s \lambda_S^s/(8\pi m_S)$, for $m_F = m_S$ and $\mu/\bar{m} = 0.15,\ 0.50$

$B/\bar{m}$	$\alpha^s_M(0.15)$	$\alpha^s_{WR}(0.15)$	$\alpha^s_M(0.50)$	$\alpha^s_{WR}(0.50)$
0.10	1.5057	1.5057	2.6558	2.6558
0.20	2.2969	2.2969	3.2644	3.6244
0.30	3.0467	3.0467	4.5354	4.5354
0.40	3.7963	3.7963	5.4505	5.4506
0.50	4.5680	4.5681	6.4042	6.4043
0.80	7.2385	7.2387	9.8789	9.8794
1.00	9.7779	9.7783	13.7379	13.7380

First column: the binding energy in unit of $\bar{m} = (m_S + m_F)/2$..
Second and fourth columns: coupling constant α_M, obtained by solving the BSE in Minkowski space, for given $B/\bar{m}$.
Third and fifth columns: Wick-rotated results, α_{WR}.

Beyond the valence ….

Sales, TF, Carlson,Sauer, PRC 63, 064003 (2001)

Marinho, TF, Pace,Salme,Sauer, PRD 77, 116010 (2008)

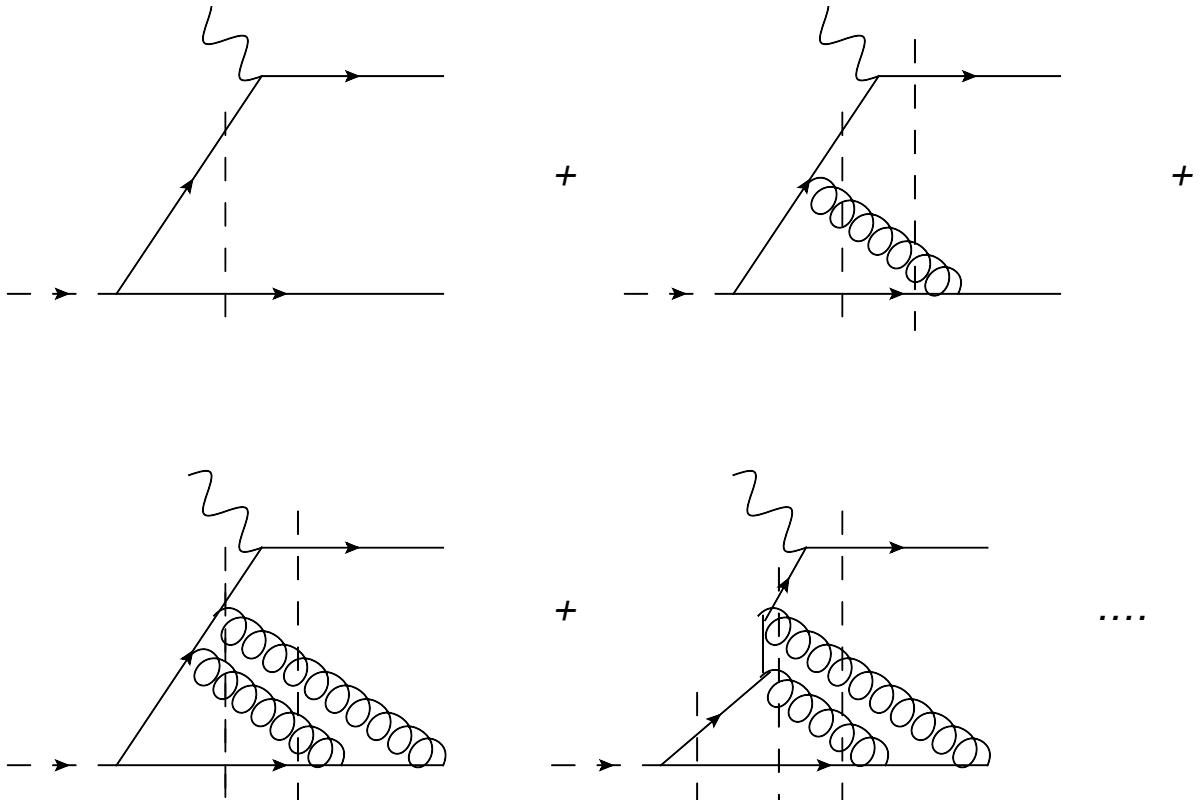

- **Population of lower x, due to the gluon radiation!**
- **Evolution?**

Beyond the valence ….

ERBL – DGLAP regions

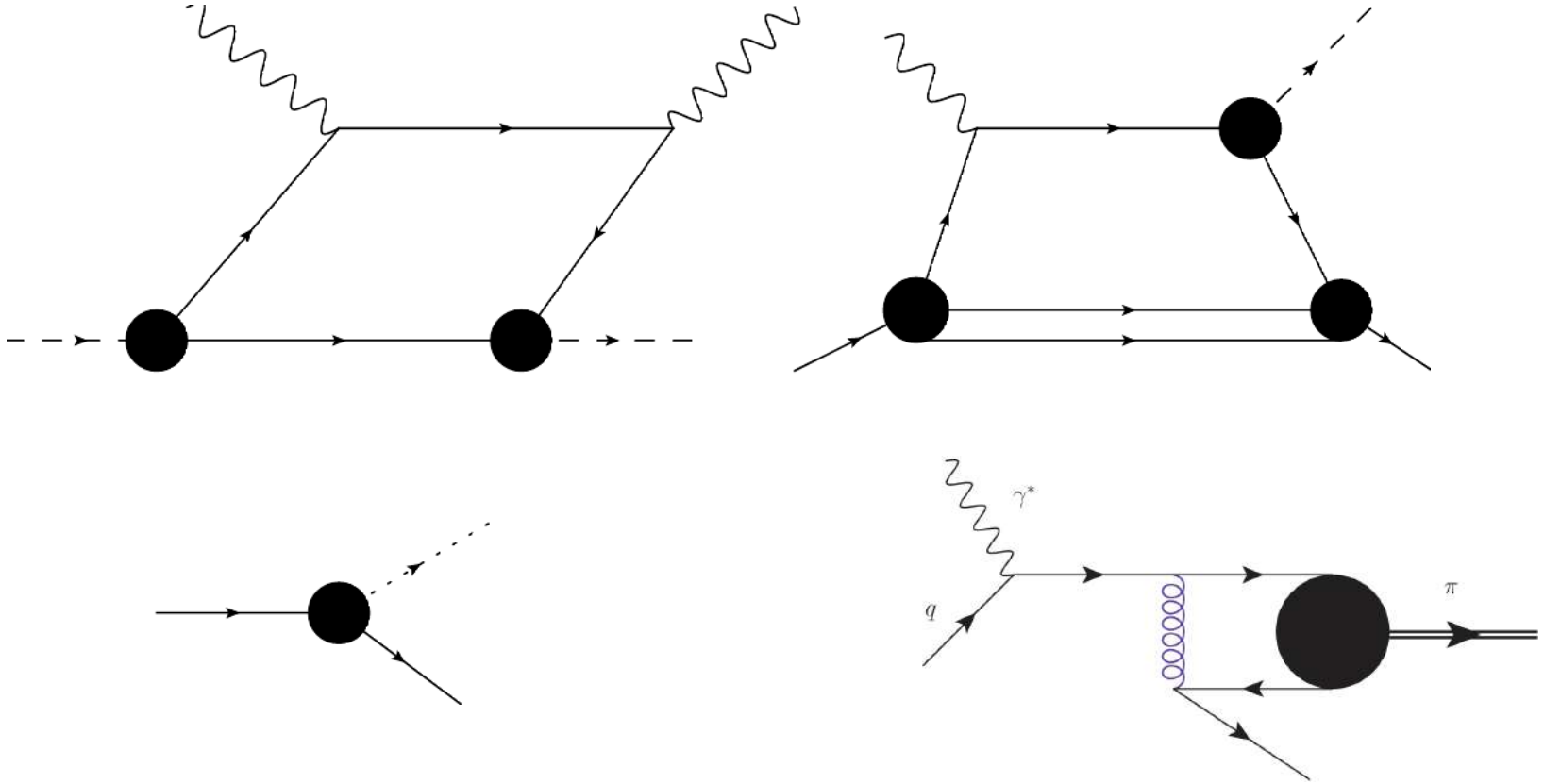

Fragmentation function

Conclusions and Perspectives

- **A method for solving the fermionic BSE: singularities**

LF framework to investigate the fermionic bound state system

- **Our numerical results confirm the robustness of the Nakanishi Integral Representation for solving the BSE.**

- **More realism: self-energies, vertex corrections, Landau gauge, ingredients from LQCD….**

- **Confinement?**

- **Beyond the pion, kaon, D, B, rho…, and the nucleon**

- **Form-Factors, PDFs, TMDs, Fragmentation Functions...**

- **Numerical Inversion of the Nakanishi weight function needs improvements…**

THANK YOU!

Analytically solvable model

$$\psi_{LF}(\gamma) = \int_0^\infty \frac{g(\gamma')d\gamma'}{(\gamma+\gamma'+1)^2}$$

we choose $z^2m^2 + \kappa^2(1-z^2) = 1$

$$g(\gamma) = \frac{1}{(1+\gamma)^2}$$

$$\psi_{LF}(\gamma) = \frac{1}{\gamma^3}\left[\frac{\gamma(2+\gamma)}{(1+\gamma)} - 2\log(1+\gamma)\right]$$

Mapping $x = \frac{\gamma}{1+\gamma}, \quad x' = \frac{\gamma'}{1+\gamma'}$

$$\psi_{LF}(x) = \int_0^1 L_1(x, x') g(x') dx'$$

$$\psi_{LF}(x) = \left[(2-x)x + 2(1-x)\log(1-x) \right] \frac{(1-x)^2}{x^3}$$

$$L_1(x, x') = \frac{1}{\left[\frac{x}{1-x} + \frac{x'}{1-x'} + 1 \right]^2} \frac{1}{(1-x')^2} = \frac{(1-x)^2}{(1-xx')^2}$$

$$g(x) = (1-x)^2.$$

Studying stability

Analytically solvable model

naive form $C_\epsilon = (A + \epsilon I)^{-1} B$

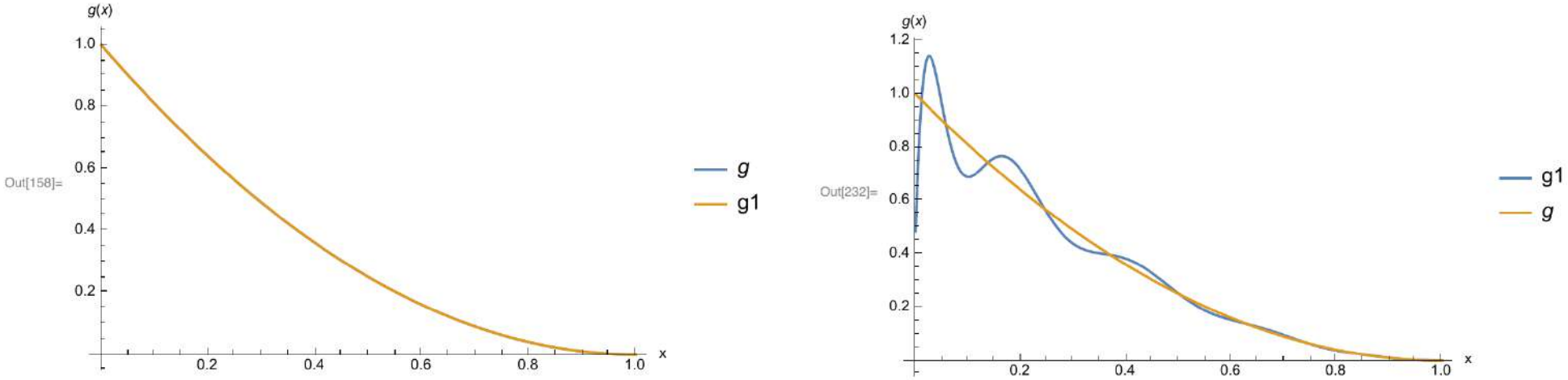

Fig. 1. The numerical solution of Eq. (22) for $g(x)$ (blue curves) with $\epsilon = 0$ in (18) for different N's found in the form of Eq. (14) in comparison to the exact solution $g(x) = (1-x)^2$ (yellow). In the left-frame the discretization rank is $N = 11$ and in the right-frame we use $N = 14$.

$$N = 11\text{: } \det(A) \sim 10^{-35}\text{; for } N = 14\text{: } \det(A) \sim 10^{-59}$$

naive form $C_\epsilon = (A + \epsilon I)^{-1} B$

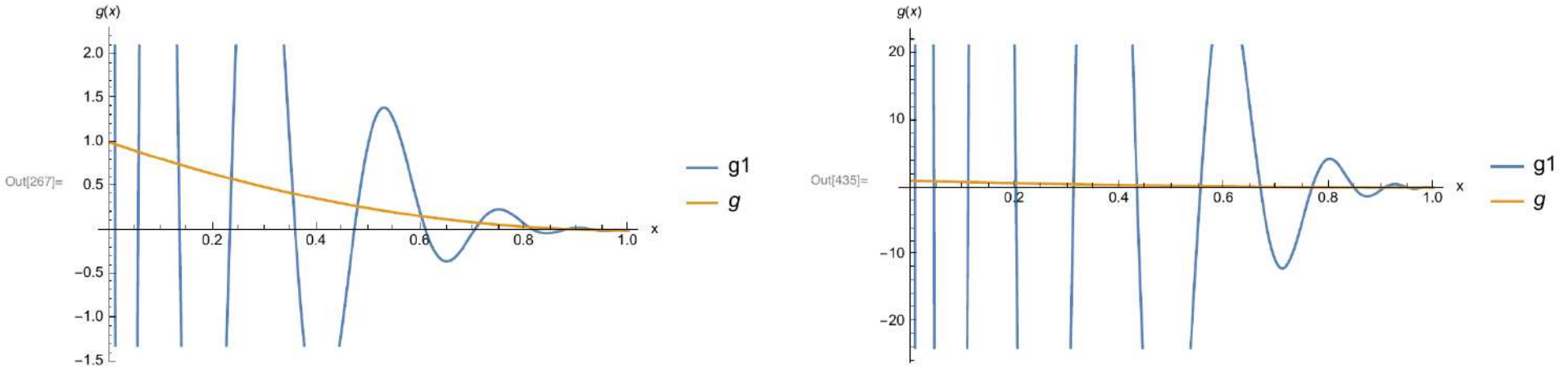

Fig. 2. The same as in Fig. 1 but for $N = 16$, $\epsilon = 0$ (left-frame), and for $N = 32$, $\epsilon = 0$ (right-frame)

Oscillations: small eigenvalues start to be relevant!

Tikhonov regularization

$$C_\epsilon = (A^\dagger A + \epsilon I)^{-1} A^\dagger B$$

$N = 16$ and $\epsilon = 10^{-10}$ $\epsilon = 10^{-4} \div 10^{-17}$

Results with the same quality

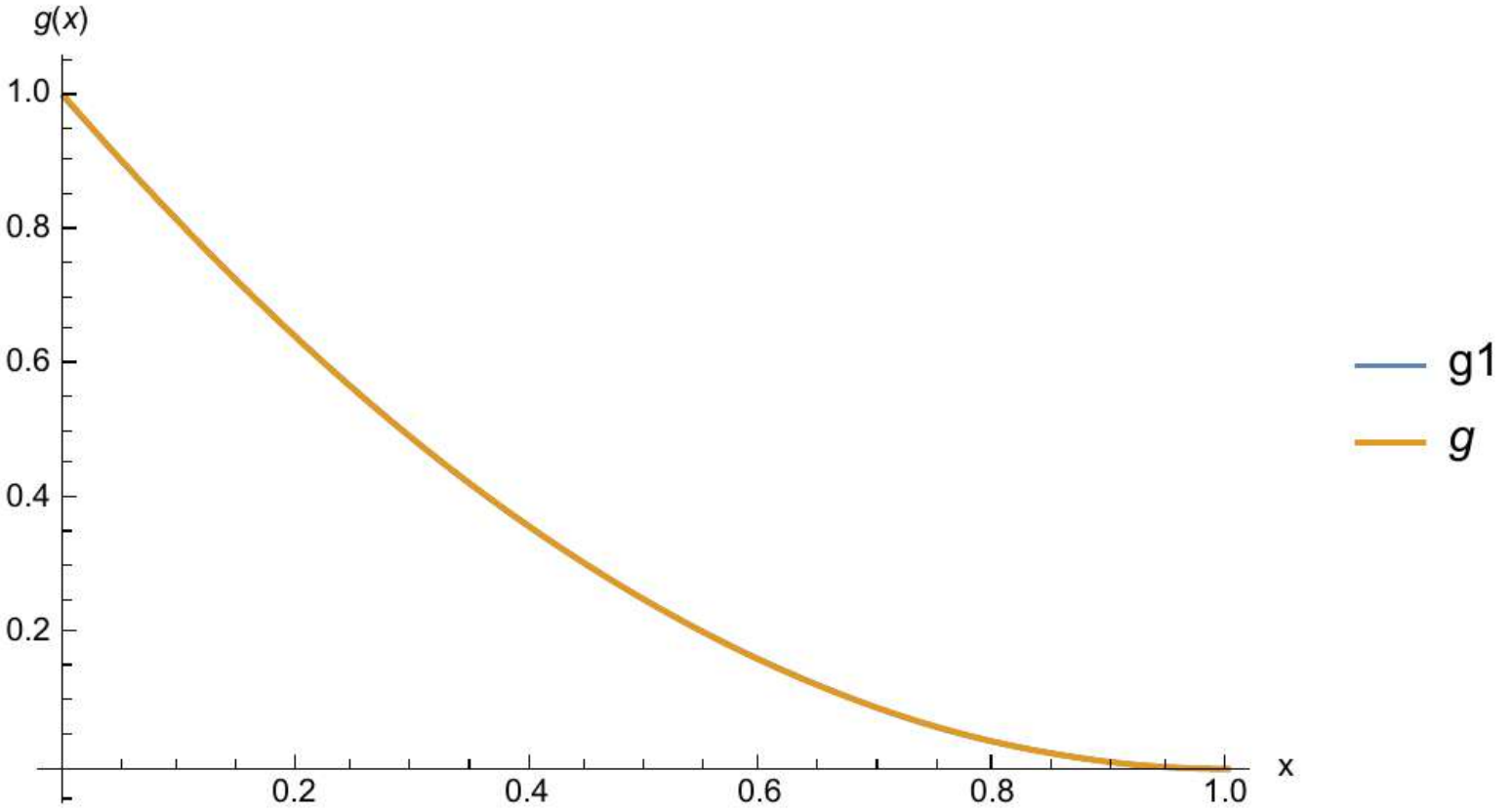

Tikhonov regularization

$$C_\epsilon = (A^\dagger A + \epsilon I)^{-1} A^\dagger B$$

$N = 16$ and $\epsilon = 10^{-10}$ Perfect match with the model

$\epsilon = 10^{-4} \div 10^{-17}$

Tikhonov regularization

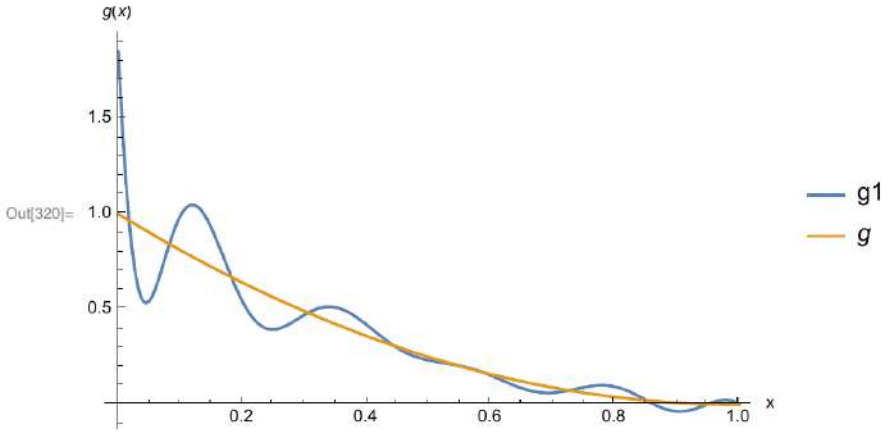

naive form

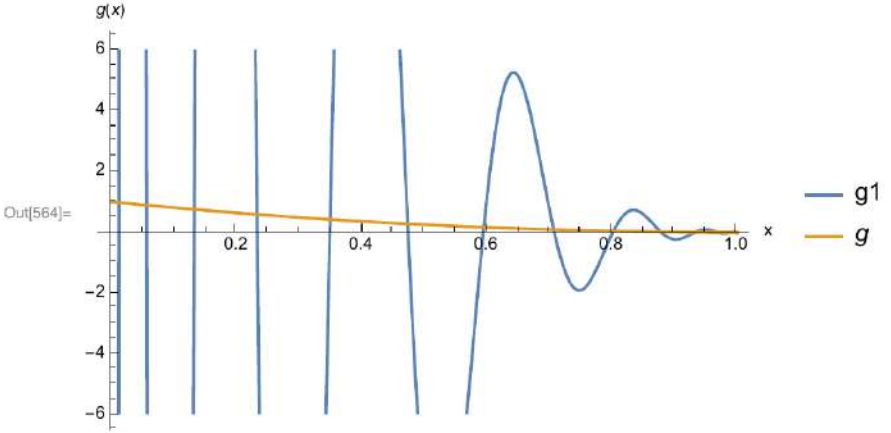

Fig. 3. The same as in Fig. 1 with Tikhonov regularization, for $N = 16$ and $\epsilon = 10^{-18}$ (left-frame). Regularization with Eq. (18) $N = 16$ and $\epsilon = 10^{-10}$ (right-frame).

$N = 32, \epsilon = 10^{-10}$ TR: match with the model

Tikhonov regularization (TRM) vs. Naive regularization

Increasing N and decreasing ε : TRM is robust

The eigenvalues for TRM larger than Naive regularization

det [TRM] >> det[Naive regularization]

Next use TRM to get g_E from the Euclidean BS amplitude

Check with LF wave function and Form Factor